AIP Journal of Applied Physics

Recombination properties of photogenerated minority carriers in polycrystalline silicon

M. R. Murti and K. V. Reddy

Citation: Journal of Applied Physics **70**, 3683 (1991); doi: 10.1063/1.349217
View online: http://dx.doi.org/10.1063/1.349217
View Table of Contents: http://scitation.aip.org/content/aip/journal/jap/70/7?ver=pdfcov
Published by the AIP Publishing

Recombination properties of photogenerated minority carriers in polycrystalline silicon

M. R. Murti and K. V. Reddy
Department of Physics, Indian Institute of Technology, Madras-600 036, India

(Received 4 February 1991; accepted for publication 8 July 1991)

An experimental investigation of the influence of grain boundaries on the recombination of photogenerated minority carriers in polysilicon is reported here. Spatial dependence of photoconductance across an isolated grain boundary was utilized to evaluate the diffusion length of electrons in the grain and the interfacial recombination velocity. Intensity dependence of these parameters provided some insight into the modulation of the grain boundary potential barrier under illumination. Photoconductance was found to vary with photon flux as G^r, where $r = 1.0$ in regions of the grain far away from the boundary and $r = 0.4$ at the grain boundary plane. The barrier height and electron capture cross section in the grain boundary traps were obtained to be 0.12 eV and 1.16×10^{-16} cm^2, respectively.

I. INTRODUCTION

In this paper we report the effect of grain boundaries on the transport of photogenerated minority carriers in polycrystalline silicon. The grain boundaries, due to their large defect state concentrations, trap majority carriers from the adjoining grains and form potential barriers. The photoconductivity in polycrystalline silicon actually traces its origin to the presence of these barriers and their modulation with illumination. The photogenerated minority carriers recombine in the grain boundary states and reduce the grain boundary potential barrier height, thereby (i) reducing the scattering losses and increasing the majority-carrier mobility and (ii) allowing a greater number of majority carriers to cross the now reduced grain boundary potential barrier. This in effect causes an increase in the conductivity of the sample. The quantity that characterizes recombination at grain boundaries is the effective recombination velocity (S) given by $J_r/[2q.\Delta n(W)]$, where J_r is the recombination current and $\Delta n(W)$ is the excess minority-carrier concentration at the edge of the depletion region.

Specific to polycrystalline semiconductors is the spatial dependence of photoconductivity/photocurrents. Originally observed by Martinez *et al.*[1] and Scholl,[2] the relative variation of photoconductivity along the sample was further investigated by Panayotatos *et al.*[3] to show that the recombination velocity at the grain boundary interface increases monotonically with the illumination intensity. Such a variation of S, however, is not in agreement with reports by other techniques such as light-/ electron-beam induced currents (LBIC and EBIC).[4–6] Depauw *et al.*[4] measured light-beam induced currents on *p-n* junctions of polysilicon and found that S decreases with increasing illumination. Detailed calculations indicated that a strong decrease of grain boundary barrier height under illumination is what is responsible for the observed decrease of recombination velocity.[6]

Here we study the spatial dependence of photovoltage (which is proportional to the photoconductivity) across an isolated grain boundary of polycrystalline silicon. Diffusion length and recombination velocity were evaluated from the response and their dependence on the illumination intensity and temperature was studied in detail. From the temperature dependence of recombination velocity, grain boundary barrier height and capture cross section for electrons in the grain boundary states were evaluated.

II. EXPERIMENTAL DETAILS

From a large grain Wacker polycrystalline silicon wafer, a sample of size $8 \times 1.5 \times 0.4$ mm was cut. The criterion for the size of the sample is that it contains, at least visibly, only one grain boundary. The samples were mechanically polished and chemically etched to get a specular, strain-free surface. Aluminium was vacuum deposited on both ends of the sample and sintered to get ohmic contacts.

The experimental arrangement for measurement of photoconductance as a function of position is shown in Fig. 1. A He-Ne laser beam was chopped mechanically and focused onto the sample as a tiny spot. An objective lens of magnification $10\times$ (numerical aperture ~ 0.22) was used to focus the beam. By scanning a knife edge across the focal plane, the diameter of the beam was determined to be ~ 20 μm. The sample was mounted on an *X-Y* platform which can be translated at a minimum step of 10 μm. A constant current was passed through the sample and care was taken to see that the voltage developed across the sample does not exceed kT/q. A signal proportional to the change in the sample conductance was measured by a PAR 124A lock-in amplifier.

By introducing calibrated neutral density filters in the path of the beam, the intensity of the incident beam could be altered by several orders. The optical density (od) of the filters used here ranged from 0.4 to 3.0. A heater placed beneath the sample served to change the temperature of the sample. Temperature variation studies were conducted in an argon atmosphere. Later, the samples were subjected to preferential etching so as to expose the grain boundaries, and optical micrographs were taken. The micrograph in Fig. 2 shows the grain boundary in one of the samples studied.

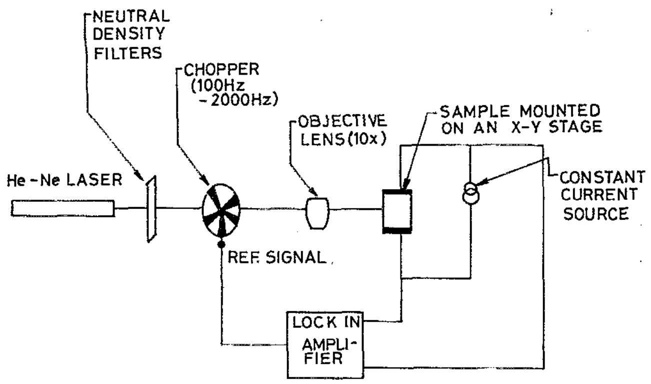

FIG. 1. Experimental setup for scanning light spot technique.

III. RESULTS AND ANALYSIS

Figure 3 shows the photovoltage (ΔV) plotted as a function of the position of light spot (with respect to the grain boundary) for different levels of illumination. It was visually observed that the peaks coincide with the position of the grain boundary. It can be seen that in regions of the grain far away from the grain boundary the response is nearly constant, whereas ΔV decreases in the near neighborhood of the boundary as one moves away from $x = 0$.

The schematic representation of the band bending near a grain boundary under dark and illuminated conditions are shown respectively in Figs. 4(a) and 4(b). Carrier transport across the grain boundary takes place via thermionic emission and the thermionic current density (J_{th}) is given by[7]

$$J_{th} \approx A^* T^2 \exp[-(E_F + qV_d)/kT] \cdot (qV_a/kT), \quad (1)$$

where A^* is the Richardson constant, E_F is the Fermi level in the bulk, V_d is the height of the grain boundary barrier, and V_a is the voltage drop across the boundary. In writing the above expression it was assumed that $V_a < kT/q$ and $V_a \ll V_d$, so that the change in the barrier height with the applied voltage is negligible. Consider that a small region of the polycrystalline sample is illuminated at a point x and electron-hole pairs are generated in excess. The excess minority carriers are transported by diffusion towards the grain boundary and are attracted by grain boundary space-charge fields into the grain boundary region, where they recombine with the trapped majority carriers. As a result, the charge in the grain boundary states is decreased as does the height of the potential barrier. The change in the thermionic current density due to barrier lowering was considered by Martinez *et al.*[1] and an expression for the photovoltage developed across the sample was given to be

$$\Delta V = \left(\frac{(bGL_n/2D_n)}{(1 + SL_n/2D_n)} \right) \times \exp(-x/L_n), \quad (2)$$

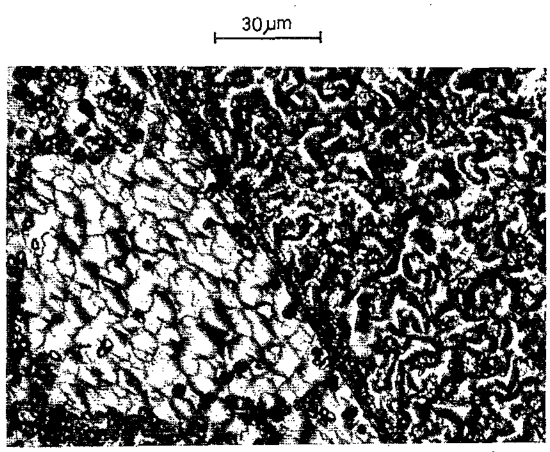

FIG. 2. Optical micrograph of the grain boundary and the adjoining grains studied in the present work (magnification = 200×). The dissimilar orientations of the grains can be seen from the photograph.

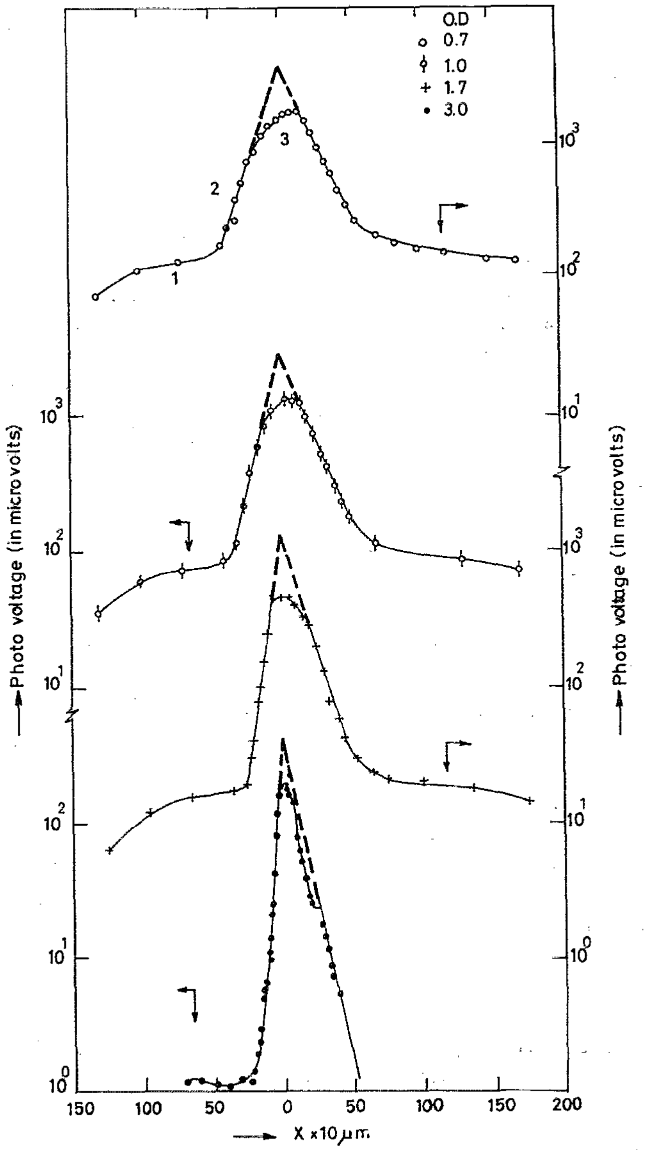

FIG. 3. Variation of photovoltage of the sample with distance from the grain boundary at different levels of illumination. (The Y axis scale for o.d. = 0.7 and 1.7 is on the right-hand side and for o.d. = 1.0 and 3.0 is on the left side).

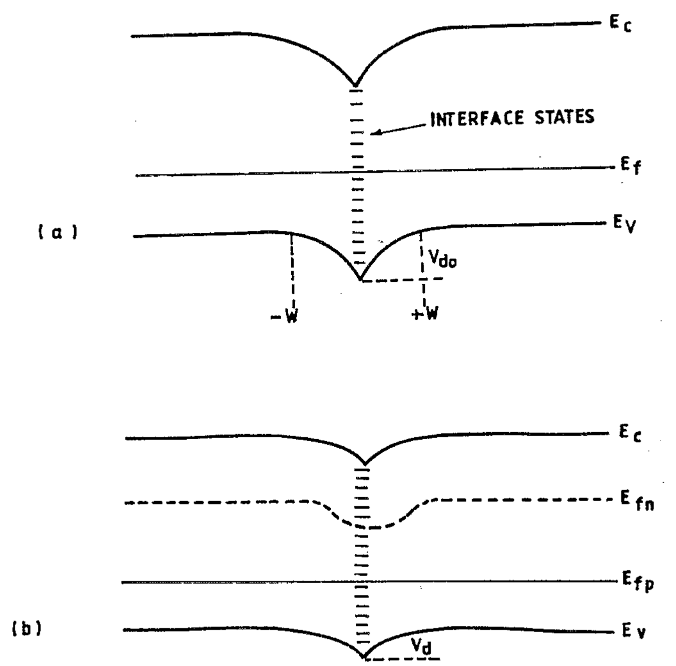

FIG. 4. Electron energy-band diagram for (a) grain boundary under dark conditions. (Grain boundary width is not shown). The dashes in the forbidden gap represent interface states. (b) Grain boundary under illumination. The Fermi level E_f splits into E_{fn} and E_{fp}.

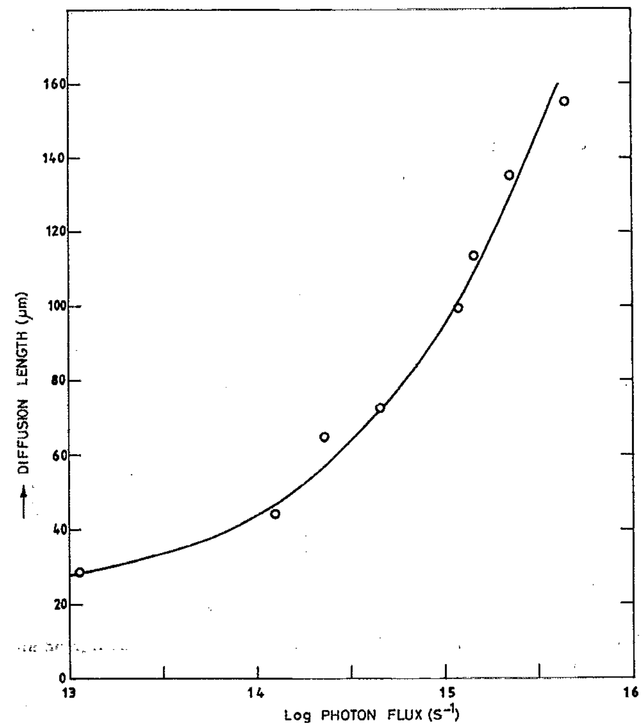

FIG. 5. Variation of diffusion length (in the grain) with photon flux.

where $b = (V_a/a) \times \exp(qV_d/kT) \times (1/p_{po})$, η = internal quantum efficiency, G = number of photons per second impinging on the surface, L_n, D_n = diffusion length and diffusion constant of minority carriers in the grain, S = recombination velocity at the gb plane, a = cross-sectional area of the sample, A^* = Richardson constant, and p_{po} = hole concentration in the bulk under dark conditions.

In regions of the grain outside the edge of the grain boundary depletion layer, bulk effects would prevail and S can be set to zero. Equation (2) thus becomes

$$\Delta V = (bGL_n/2D_n)\exp(-x/L_n). \quad (3)$$

It can be seen from Fig. 3 that $\log \Delta V$ varies linearly with x on either side of the boundary in accordance with Eq. (3). L_n was obtained from the slope and plotted against the photon flux in Fig. 5. It can also be seen from Fig. 3 that close to the boundary $\log \Delta V$ departs from linearity and the peak at $x=0$ is either flat or rounded. The departure from linearity is an indication of the fact that $S \neq 0$ here. Recombination velocity can be obtained by a method due to Panayotatos *et al.*[3] and is described below. If there was no recombination at the boundary (i.e., $S=0$), bulk effects would have continued to prevail and the photoresponse in Fig. 3 would have continued to increase up to the point $x=0$. The photovoltage in such a case is given by setting $S=0$ and $x=0$ in Eq. (2) as

$$\Delta V'(0) = bGL_n/2D_n. \quad (4)$$

However, in the actual case where $S \neq 0$ and

$$\Delta V(0) = \left(\frac{(bGL_n/2D_n)}{(1+SL_n/2D_n)}\right), \quad (5)$$

$\Delta V'(0)$ is obtained by extrapolating the linear regions in Fig. 3 to $x=0$. The ratio of the observed value of photovoltage to that obtained by extrapolation is given by

$$\frac{\Delta V(0)}{\Delta V'(0)} = \left(\frac{1}{(1+SL_n/2D_n)}\right). \quad (6)$$

Since L_n and D_n ($=25\ \text{cm}^2\,\text{s}^{-1}$) are known in the above equation, S was calculated from the photovoltage profiles and is plotted against photon flux in Fig. 6. The photoresponse profiles were obtained for different temperatures and were analyzed to get L_n and S. Figure 7 shows the recombination velocity plotted against $10^3/T$.

Since diffusion takes place from the outer edge of the light spot to the surrounding regions, it appears that the spot size is not of considerable importance for measurements in the bulk of the grain. However as the grain boundary is approached, the material displays nonuniformities, and so it is advisable to have extended photoresponse scans along the sample with smaller spot sizes and smaller translational step widths. To minimize the errors it was suggested that the spot size should be less than the diffusion length and the grain size.[3,8] Care was taken to meet these conditions in our experiment.

IV. DISCUSSION

A. Dependence of L_n and S on illumination level

The photoresponse profiles in Fig. 3 suggest that polycrystalline samples in general and bicrystals in particular

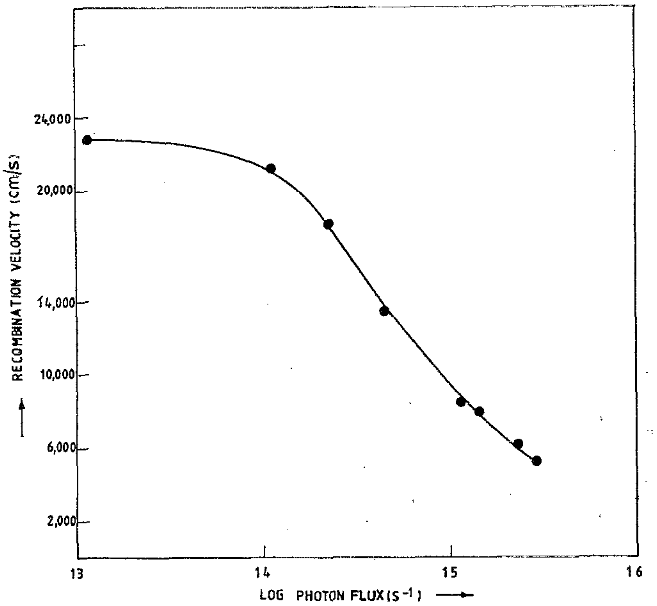

FIG. 6. Variation of grain boundary recombination velocity with incident photon flux.

can be treated as being composed of three regions as designated in the figure. In regions of the grain far away from the boundary (region 1), the photovoltage ($\Delta V_{\min}$) is nearly independent of position. However, $\Delta V_{\min}$ (taken at $x = -700$ μm) was found to vary with photon flux as G^r where $r \sim 1$ as shown in Fig. 8(a). Such a relationship, as is well known, characterizes the low injection conditions in single crystals where the photoconductivity increases proportionately with the excess minority-carrier concentration.

Within a few diffusion lengths from the grain boundary, it can be seen that photovoltage increases as the boundary is approached (region 2). The variation of L_n, with photon flux obtained from this region, indicates that the diffusion length in the grain is affected by the presence of the grain boundary barrier and its modulation under light. As the light spot approaches the grain boundary, the population of minority carriers reaching and recombining in the grain boundary region increases exponentially, thus causing a reduction in barrier height and hence an increase

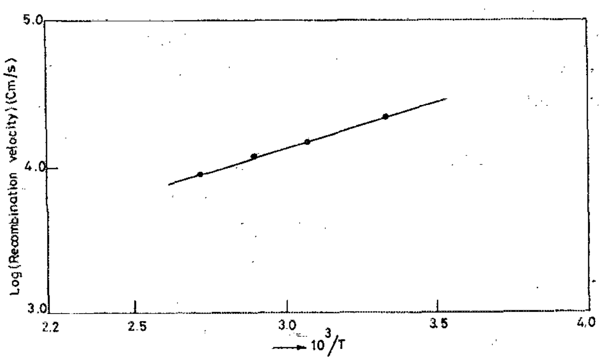

FIG. 7. Temperature dependence of recombination velocity at the grain boundary interface for constant intensity of illumination (o.d. = 2.0)

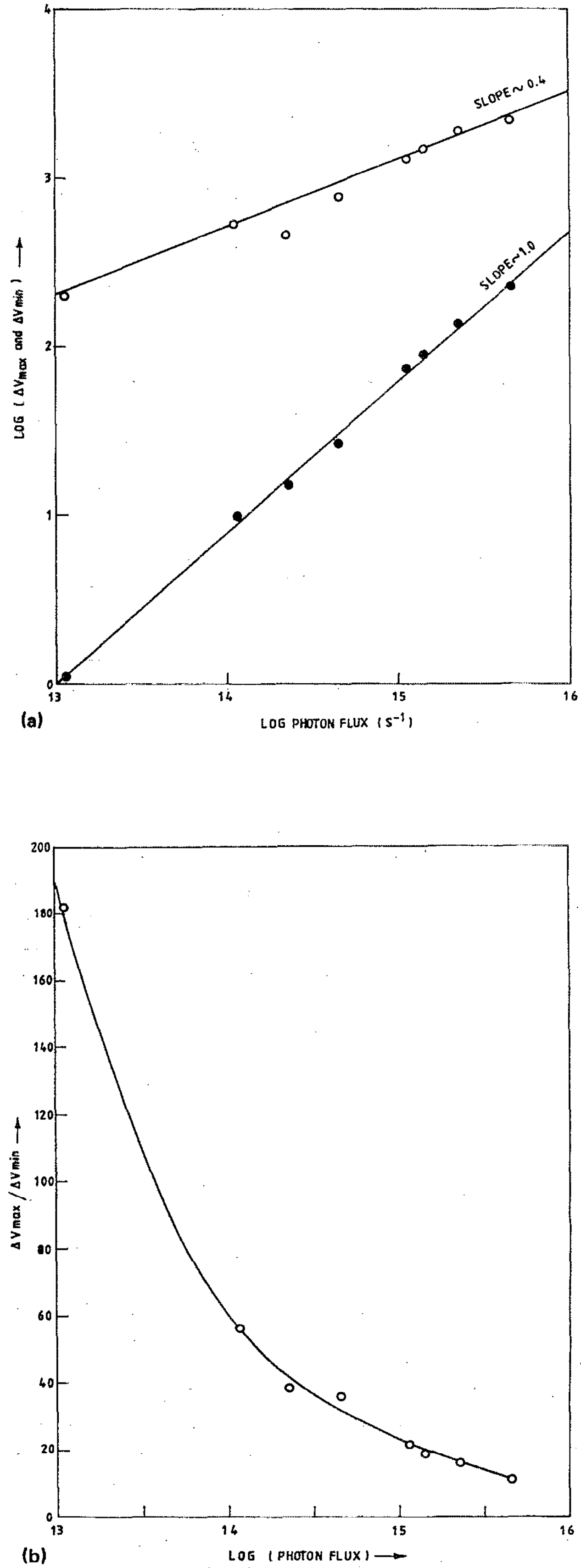

FIG. 8. (a) Variation of $\Delta V_{\max}$ (at $x = 0$) and $\Delta V_{\min}$ (at $x = -700$ μm) as a function of photon flux. (○) $\Delta V_{\max}$ and (●) $\Delta V_{\min}$. (Data from Fig 3 is plotted). (b) Variation of $\Delta V_{\max}/\Delta V_{\min}$ with incident photon flux.

in the photovoltage. The effective minority-carrier lifetime in this region may thus be written as

$$\frac{1}{\tau_{\text{eff}}}=\frac{1}{\tau_g}+\frac{1}{\tau_{\text{gb}}}, \tag{7}$$

where τ_g is the lifetime in the grain and τ_{gb} is that in the grain boundary region. τ_{gb} is dominated by recombination in the grain boundary region and is thus a function of illumination. The effect of illumination is to increase τ_{eff} through the increase of τ_{gb}, and τ_{eff} approaches τ_g at higher illumination levels. This is reflected in the observed behavior of L_n in Fig. 5.

In the region encompassing the grain boundary (region 3), the photoresponse is suppressed (shown by rounded or depressed peaks) indicating that the recombination velocity is finite. The band bending at the grain boundary enhances the minority-carrier excesses by a factor of $\exp(qV_d/kT)$ and makes them available for recombination. This lowers the net charge stored in the grain boundary region and hence the barrier height. The lowering of the barrier counteracts the increase of $n_p(0)$ and the recombination current. As a result, the recombination velocity S decreases with increasing illumination level. Thus polysilicon solar cells are expected to be more efficient at higher levels of illumination. Also it was found that $\Delta V_{\max}$ (taken at $x=0$) varies with photon flux as G^r where $r=0.4$ [Fig 8(a)]. Such a power law variation of photoconductivity is not new for disordered semiconductors and actually indicates that the density of grain boundary states is distributed continuously in the forbidden gap.[9]

B. Temperature dependence of recombination velocity

Spatial profiles of the photoresponse were obtained at different temperatures above 300 K and L_n and S were calculated. It was found that the photovoltage at a given distance is smaller at higher temperatures, while L_n decreased with increasing temperature. As the temperature is raised, a greater number of carriers can cross the grain boundary barrier by virtue of their increased thermal energy. However, the probability of carriers being captured in the grain boundary states is less than what it were at a lower temperature. Consequently, the contribution to photovoltage from barrier height modulation decreases with increasing temperature. Because the recombination probability has decreased, τ_{eff} would have increased with temperature and hence the diffusion length. For the same reason, recombination velocity also decreases with temperature.

The effective recombination velocity under equilibrium conditions is related to the grain boundary barrier height as[10]

$$S=\sigma v_{\text{th}}(2\epsilon\epsilon_0 N_a\cdot V_d/q)^{1/2}\exp(qV_d/kT), \tag{8}$$

where σ is the capture cross section of grain boundary hole traps for capturing an electron, v_{th} is the thermal velocity of electrons, N_a is the acceptor dopant concentration in the material, ϵ is the permittivity of polysilicon, and ϵ_0 is the permittivity of vacuum. This expression was derived for steady-state conditions when the flux of minority carriers down the potential gradient was balanced by a flux of majority carriers to the vacant interface states.

In accordance with Eq. (8), $\log S$ was found to vary linearly with $1/T$ (Fig. 7) and the slope and intercept were utilized to evaluate the barrier height and capture cross section. They were obtained to be 0.12 eV and $1.16\times10^{-16}\,\text{cm}^2$, respectively. This value of V_d corresponds to the barrier height under dark conditions.

C. Sensitivity of the barrier for illumination

It is discernible from Fig. 8(b) that the barrier is more sensitive to light at lower illumination levels: $(\Delta V_{\max}/\Delta V_{\min})$ was found to decrease with photon flux as $\sim G^{-0.6}$. In other words grain boundaries with larger barrier height show greater sensitivity to illumination—this corroborates with the studies of Seager[10] and McGonigal *et al.*[11] who investigated silicon bicrystals of varying barrier height under fixed illumination. At low illumination levels, since the barrier height is large and the hole concentration at the grain boundary varies as $p\sim\exp(-qV_d/kT)$ the barrier must be substantially modulated to supply excess holes needed for recombination with the collected electrons. For small barriers sufficient holes become available even for minor modulation of the barrier.

It is the nature of the grain boundaries in semiconductors, in general, that the barrier height attributed to them shows local variations even in a given grain boundary. These variations are a result of the various kinds of disorder that a grain boundary is made up of, namely dangling bonds, distorted bonds, and impurity segregation at the grain boundary interface. These fluctuations in V_d have been studied both experimentally[1,12] as well as theoretically[13] by several authors. In light of this, it may be mentioned that the V_d value obtained above is valid for the region of the particular boundary studied here. Also more direct measurements such as photocapacitance[14] and current-voltage (I-V) characteristics of a grain boundary[11] will help in unraveling the detailed distribution of grain boundary states in polysilicon.

V. CONCLUSIONS

Photoconductance measurements in polycrystalline silicon were used to derive information about the influence of grain boundaries on minority-carrier transport. The decrease of grain boundary barrier height under illumination has resulted in an increase of minority-carrier diffusion length in the regions of the grain nearer the grain boundary. Recombination velocity at the grain boundary interface was found to be highest at low illumination levels.

The photoresponse was found to vary with photon flux as G^r, where $r=1.0$ far away from the boundary and $r=0.4$ at the grain boundary plane. The sublinear variation suggests that the grain boundary states are distributed continuously in the gap. It was also found that the grain boundary was most sensitive to light under low levels of illumination.

The temperature dependence of recombination velocity was utilized to obtain the unmodulated grain boundary barrier height and capture cross section of trap states.

ACKNOWLEDGMENTS

The authors wish to thank Professor Y. V. G. S. Murty for extending to us the use of his laboratory facilities.

[1] J. Martinez, A. Criado, and J. Piqueras, J. Appl. Phys. **52**, 1301 (1981).
[2] F. W. Scholl, J. Appl. Phys. **52**, 3439 (1981).
[3] P. Panayotatos, E. S. Yang, and W. Hwang, Solid State Electron, **5**, 417 (1982).
[4] P. Depauw, R. Mertens, R. Van Overstraeten, and K. U. Leuven, IEEE Electron Device Lett. **EDL-5**, 234 (1984).
[5] C. H. Seager, J. Appl. Phys. **53**, 5968 (1982).
[6] C. Donolato and R. O. Bell, Rev. Sci. Instrum. **54**, 1005 (1983).
[7] J. Y. W. Seto, J. Appl. Phys. **46**, 5247 (1975).
[8] J. Oualid, C. M. Singal, J. Dugas, J. P. Crest, and H. Amzil, J. Appl. Phys. **55**, 1195 (1984).
[9] A. Rose, *Concepts in Photoconductivity and Allied Problems* (Kreiger, Huntington, NY, 1963), p. 38.
[10] C. H. Seager, J. Appl. Phys. **52**, 3960 (1981).
[11] G. C. McGonigal, D. J. Thomson, J. G. Shaw, and H. C. Card, Phys. Rev. B **28**, 5908 (1983).
[12] Y. Alpern and J. Shappir, J. Appl. Phys. **63**, 2964 (1988).
[13] D. J. Thomson and H. C. Card, J. Appl. Phys. **54**, 1976 (1983).
[14] J. Werner, W. Janisch, and Q. J. Queisser, Solid State Commun. **42**, 415 (1982).